Title
A preliminary safety assessment of vertebral augmentation with 32P brachytherapy bone cement

Journal
Physics in Medicine and Biology, 67(7)

ISSN
0031-9155

Authors
Keyak, Joyce H
Eijansantos, Mando L
Rosecrance, Katherine G
et al.

Publication Date
2022-04-07

DOI
10.1088/1361-6560/ac5e5d

Peer reviewed

A Preliminary Safety Assessment of Vertebral Augmentation with ^{32}P Brachytherapy Bone Cement

Joyce H. Keyak[1,2,3,4], Mando L. Eijansantos[1], Katherine G. Rosecrance[5], Daniel Wong[1], Sayeh Feizi[2], Aleen L. Meldosian[2], Pranav Peddinti[3], Clifford M. Les[6], Harry B. Skinner[7,8], and Varun Sehgal[9]

May 12, 2022

[1] Department of Radiological Sciences, University of California, Irvine, CA, USA

[2] Department of Biomedical Engineering, University of California, Irvine, CA, USA

[3] Department of Mechanical and Aerospace Engineering, University of California, Irvine, CA, USA

[4] Chao Family Comprehensive Cancer Center, University of California, Irvine, CA, USA

[5] School of Medicine, University of California, Irvine, CA, USA

[6] Pedicaris Research, PLLC, Citrus Heights, CA, USA

[7] Bone-Rad Therapeutics, Inc., Corona del Mar, CA, USA

[8] St. Jude Heritage Medical Group, Fullerton, CA, USA

[9] Department of Radiation Oncology, University of California Irvine Medical Center, Orange, CA, USA

E-mail: jhkeyak@hs.uci.edu

Keywords: brachytherapy, metastatic bone disease, bone cement, vertebral augmentation, radiation, spine, cancer

Abstract

Comprehensive treatment for vertebral metastatic lesions commonly involves vertebral augmentation (vertebroplasty or kyphoplasty) to relieve pain and stabilize the spine followed by multiple sessions of radiotherapy. We propose to combine vertebral augmentation and radiotherapy into a single treatment by adding ^{32}P, a β-emitting radionuclide, to bone cement, thereby enabling spinal brachytherapy to be performed without irradiating the spinal cord. The goal of this study was to address key dosimetry and safety questions prior to performing extensive animal studies. The ^{32}P was in the form of hydroxyapatite powder activated by neutron bombardment in a nuclear reactor. We performed ex vivo dosimetry experiments to establish criteria for safe placement of the cement within the sheep vertebral body. In an in vivo study, we treated three control ewes and three experimental ewes with brachytherapy cement containing 2.23 mCi ^{32}P/mL to 3.03 mCi ^{32}P/mL to identify the preferred surgical approach, to determine if ^{32}P leaches from the cement and into the blood, urine, or feces, and to identify unexpected adverse effects. Our ex vivo experiments showed that cement with 4 mCi ^{32}P/mL could be safely implanted in the vertebral body if the cement surface is at least 4 mm from the spinal cord in sheep and 5 mm from the spinal cord in humans. In vivo, a lateral retroperitoneal surgical approach, ventral to the transverse processes, was identified as easy to perform while allowing a safe distance to the spinal cord. The blood, urine, and feces of the sheep did not contain detectable levels of ^{32}P, and the sheep did not experience any neurologic or other adverse effects from the brachytherapy cement. These results demonstrate, on a preliminary level, the relative safety of this brachytherapy cement and support additional development and testing.

1. Introduction

The spine is the most frequent site of bony metastasis (Hage *et al* 2000), and metastatic spine lesions are known to occur in 30% – 50% of all cancer patients (Wong *et al* 1990, Harel and Angelov 2010). Rates of spinal metastases vary by primary cancer type, with the highest rates noted in 74% – 79% of breast cancer patients and 90% of prostate cancer patients at autopsy (Wong *et al* 1990, Budczies *et al* 2014). Vertebral lesions and secondary skeletal related events, e.g. pathologic fracture and spinal cord compression, correlate with shorter survival and cause significant pain, loss of functional status, and decreased quality of life (Hernandez *et al* 2018, Barzilai *et al* 2019).

Comprehensive treatment for vertebral metastatic lesions most commonly involves vertebral augmentation (vertebroplasty or kyphoplasty) to relieve pain and stabilize the spine followed by radiation therapy. Vertebral augmentation has been shown to decrease pain, improve or maintain mobility, and improve quality of life (Mendel *et al* 2009, Berenson *et al* 2011). Studies demonstrate 73% – 85% of patients experienced moderate-to-complete pain relief following vertebral augmentation (Georgy 2008). Radiation can be administered through traditional external beam radiation therapy (EBRT) or, more recently developed and more costly, intensity modulated radiation therapy (IMRT) or stereotactic body radiation therapy (SBRT). EBRT, IMRT and SBRT reduce pain from the lesion and control disease progression (Harel and Angelov 2010, Barzilai *et al* 2019). EBRT is typically delivered in multiple small doses (treatment fractions) over two or more weeks to limit toxicity to anatomical structures in close proximity to the lesion, such as the spinal cord. IMRT and SBRT offer more localized radiation, potentially with fewer treatment fractions and increased efficacy against radioresistant tumors which may not respond to EBRT (Barzilai *et al* 2019). However, even SBRT can require up to

five treatment fractions, and dose is limited by risk of myelopathy with positional deviations of 1-2 mm significantly increasing unintentional radiation to the spinal cord (Sahgal *et al* 2013). Whether radiotherapy is administered as EBRT, IMRT or SBRT, each therapy session can be associated with side effects such as nausea, vomiting or diarrhea due to irradiation of the gastrointestinal tract. The poor bone quality associated with vertebral metastases is also further degraded by the effects of radiotherapy, with occurrence or progression of vertebral body compression fracture noted in less than 5% of patients receiving EBRT but 5.7% to 39% of patients treated with IMRT or SBRT, depending on dose and fractionation (Rose *et al* 2009, Husain *et al* 2017, Virk *et al* 2017, Rich *et al* 2018, Barzilai *et al* 2019, Zeng *et al* 2019). Together, the current treatment regimen of vertebral augmentation to stabilize the spine followed by radiation therapy still poses the inconvenience of multiple treatment sessions and associated side effects for patients and their caregivers and results in extensive use of healthcare facilities.

As an alternative to the conventional two-phase treatment for metastatic tumors in the vertebral body, we propose performing vertebral augmentation with a bone cement containing ^{32}P, a β-emitting radionuclide with a 14.3-day half-life (Kaneko *et al* 2010, Kaneko *et al* 2012). This procedure would combine local radiation therapy and vertebral augmentation into a single treatment, i.e. spinal brachytherapy, offering stabilization and early pain relief while providing local tumor control. Additional advantages of spinal brachytherapy with ^{32}P are a higher radiation dose to the adjacent bone and tumor, a lower radiation dose to the spinal cord, and essentially no radiation to the gastrointestinal tract, eliminating the nausea, vomiting and diarrhea of conventional radiotherapy, ultimately improving the quality of life for these patients.

To determine if treatment with ^{32}P brachytherapy bone cement would be feasible, we developed and verified models to estimate the dose distribution in human vertebrae and

demonstrated through simulated scenarios that ^{32}P brachytherapy cement could deliver therapeutically relevant radiation doses while sparing the spinal cord (Kaneko *et al* 2010, Kaneko *et al* 2012). We also found that the dose from ^{32}P brachytherapy cement depends on the activity concentration (mCi/mL) of the cement and the perpendicular distance from the cement surface, but not on the volume of bone cement implanted, i.e. the total activity implanted, if the cement is at least 2 mm thick (Kaneko *et al* 2012, Keyak *et al* 2015). This behavior stems from the self-shielding nature of the cement, preventing emissions more than about 2 mm below the cement surface from leaving the cement. The result is that the dosimetry associated with this brachytherapy cement is simpler than that for conventional brachytherapy seeds. However, questions about our brachytherapy cement remain unanswered.

The goal of the present study was to answer key questions prior to performing extensive studies in vivo in sheep, the animal model that is typically used for vertebral augmentation research due to anatomical similarities between sheep and human vertebrae (Liebschner 2004). Specifically, we performed ex vivo dosimetry experiments to establish the criteria for safe placement of ^{32}P bone cement in the sheep vertebral body relative to the spinal cord and soft tissues outside the vertebral body, such as peripheral nerves, and we performed an in vivo study to assess the preferred surgical approach, to determine if ^{32}P leaches from the cement into the bloodstream, or is found in the urine or feces, and to identify any unexpected adverse effects from the cement that would potentially influence translation of brachytherapy bone cement to clinical use.

2. Methods

2.1 Production of ^{32}P and Cement Preparation

The ^{32}P component of the brachytherapy cement was provided in the form of hydroxyapatite powder (HAP) that had been activated by bombardment with neutrons in a nuclear reactor to create ^{32}P-HAP. This compound was chosen because hydroxyapatite exhibits very low solubility in water. Due to the presence of calcium in the hydroxyapatite, calcium radioisotopes were also formed, but with negligible effect on dosimetry.

For each batch of cement, a fused silica vial containing 0.340 g HAP was sealed under vacuum. For the ex vivo studies, two vials were placed in the core of a nuclear reactor (TRIGA™, General Atomics) located at McClellan Nuclear Research Center, Sacramento, CA, USA, for 113 hours at 1 MW power over a three-week period (7-8 hours per day, Monday through Friday). One of these vials was used in cement for dosimetry experiments and the other, the "Calibration Vial", was used to calibrate a dose calibrator (CRC-55tW Dose Calibrator and Well Counter, Capintec, Inc.), as described in the Appendix. For the in vivo studies, two or three vials at a time were placed in the reflector of a nuclear reactor for 146 to 155 hours continuously (Missouri University Research Reactor, Columbia, MO, USA). Each vial was then placed in the dose calibrator to obtain a provisional measurement of the ^{32}P activity in the vial. Once the dose calibrator was calibrated, the provisional measurement of the ^{32}P activity in each vial was multiplied by a scaling factor to obtain the actual ^{32}P activity in each vial (see Appendix).

Preparation of each batch of brachytherapy cement involved adding an entire vial of ^{32}P-HAP to one 20-g dose of sterile bone cement powder (Kyphon HV-R, Medtronic, Inc.) and mixing the powders with a 9-g ampoule of sterile liquid cement monomer (Kyphon HV-R,

Medtronic, Inc.) for 90 seconds using a cement mixer (Minimix CMM4, IZI Medical). The mixed radioactive bone cement was then transferred to a 3 mL polyethylene/polypropylene syringe (Norm-Ject, Henke Sass Wolf, Germany) fitted with a 10-gauge stainless steel blunt needle with a nickel-plated brass hub (Hamilton Company).

Exposure of personnel to the high-energy ^{32}P emissions was minimized by using tools to increase distance to the radioactive material, providing polypropylene and polycarbonate shielding, and minimizing time close to the material. For the in vivo experiments, the ^{32}P-HAP vial was sterilized using dry heat sterilization and all tools and shielding were autoclaved. Containment of the ^{32}P-HAP while opening the vial and mixing the cement was achieved by placing the vial into a sealed sterile plastic bag that was attached to the top of the cement mixer. The plastic bag also contained the liquid monomer ampoule and the cover to the cement mixer.

2.2. Ex Vivo Dose Measurements

Ex vivo experiments were performed to measure the radiation dose that would be delivered to the spinal cord and adjacent soft tissues after performing kyphoplasty with ^{32}P cement in an ovine model. Radiation dose was measured using radiochromic film (GAFChromic EBT3, Ashland, Inc.). This film is composed of 2 outer polyester layers and an inner active layer that produces a color change dependent on radiation dose.

Six vertebrae (L1-L6) were obtained from a cadaveric sheep (Rambouillet X Columbia ewe) after sacrifice from one of several ongoing ovine studies that examined questions not relevant to our work and that were approved by the University of California, Irvine (UCI) Institutional Animal Care and Use Committee (IACUC). A hole was drilled mediolaterally into the lateral aspect of each vertebral body, near the cranial or caudal end, using a 5.2-mm-diameter

cannulated drill bit (Figure 1). The dose at the ventral surface of the spinal canal was assumed to be the dose to the ventral surface of the spinal cord, and the distance from that surface to the closest part of the drill hole was different in each vertebra so that a range of doses would be measured. This distance was not directly visible but could be measured with reasonable accuracy (within about 0.5 mm) using calipers, with the drill bit inserted, and was approximately 1 mm, 2.5 mm, 3 mm, 4 mm, 5 mm, and 6 mm for the six drill holes. To allow for radiochromic film to be placed on the ventral surface of the spinal canal, the dorsal vertebral arch was removed with an oscillating saw by cutting through the lamina, adjacent to the medial aspect of each facet. The spinal cord was removed, and a piece of radiochromic film was placed on the ventral surface of the spinal canal and held in place with elastic bands (Figure 1). Brachytherapy bone cement containing 0.267 mCi ^{32}P/mL was injected into the hole in each vertebral body by placing the needle against the bottom of the hole and gradually injecting the cement while withdrawing the needle to prevent air from becoming trapped in the hole. The pieces of radiochromic film placed 0.5 mm to 4 mm from the cement were removed from the specimens 23 h to 34 d after injection of the radioactive bone cement, when doses within the optimal range for the film (0.2-10 Gy) were delivered. Two pieces of film 5 mm and 6 mm from the cement were exposed for 181 d.

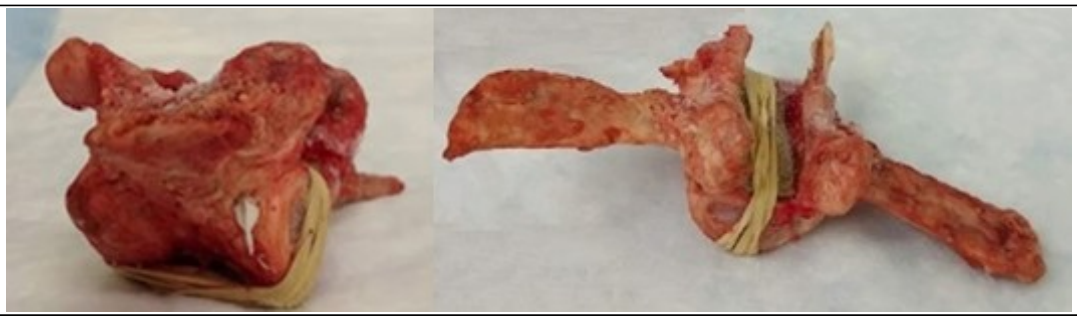

Figure 1. A hole was drilled into the vertebral body to receive brachytherapy cement (left). The spinous processes were removed, enabling placement of radiochromic film on the ventral surface of the spinal canal (right).

To evaluate the dose delivered to soft tissue adjacent to brachytherapy cement, the same batch of cement containing 0.267 mCi ^{32}P/mL was used to create cement disks measuring 12.7 mm in diameter and at least 6 mm high by injecting cement into polypropylene molds. After removing the bottom of the mold, each radioactive disk surrounded by its polypropylene mold was placed atop a sheet of polycarbonate measuring from 1.1 mm to 5.45 mm thick to simulate the effect of soft tissue of varying thickness. Radiochromic film was placed under each polycarbonate sheet for 3 h to 23 d, until 0.2-10 Gy was delivered. Our previous work showed that, aside from edge effects near the perimeter of the disk, the dose from ^{32}P brachytherapy cement to the film depends only on the activity concentration and the perpendicular distance from the cement surface, and not the total activity or thickness of the cement, if the cement is at least about 2 mm thick (Kaneko *et al* 2012, Keyak *et al* 2015). Therefore, the dose measured beneath the center portion of each disk (at least 2-3 mm from the edge of the disk) would be the same even if the thickness of the disk varied.

2.3. Processing radiochromic film

To calibrate the radiochromic film, twelve pieces of film were exposed to 0.0, 0.10, 0.20, 0.40, 0.80, 1.6, 2.4, 3.2, 4.6, 6.0, 8.0, and 10.0 Gy, respectively, using a 12 MeV electron beam from a linear accelerator (Clinac 21-EX, Varian Medical Systems, Inc.). After exposure, all film,

including film for calibration and film used to measure dose, was allowed to stabilize for at least 24 hours, scanned at 150 dpi with consistent orientation using a flatbed scanner (EPSON Expression 11000XL Photo scanner), and processed by a Matlab script (Mathworks, Inc.). Using a triple-channel approach (Micke *et al* 2011, Palmer *et al* 2014), the red, blue, and green pixel intensities were converted to their respective optical densities.

The average optical density of each calibration film was calculated. For each color channel, a calibration equation of the following form was obtained between the known radiation dose and the average optical density: $OD = a + b/(D - c)$, where a, b, and c are constants, OD is the optical density, and D is the known radiation dose (EBT3 Specification and User Guide).

To process the film that was used to measure dose, the optical density at each pixel was obtained for each of the red, blue, and green color channels (Figure 2), and a 3x3 mean filter was applied. From the filtered optical densities, the dose at each pixel for each color channel was calculated using the respective calibration equation. The doses from the three color channels were then averaged to obtain the measured pixel dose, and the maximum measured pixel dose was identified. From the maximum measured pixel dose and the exposure time, the maximum lifetime dose was calculated using standard decay equations. Our previous work (Kaneko *et al* 2012, Keyak *et al* 2015) showed that the dose from radioactive bone cement depends on the activity concentration (mCi/mL), so the maximum lifetime dose was normalized to activity concentration.

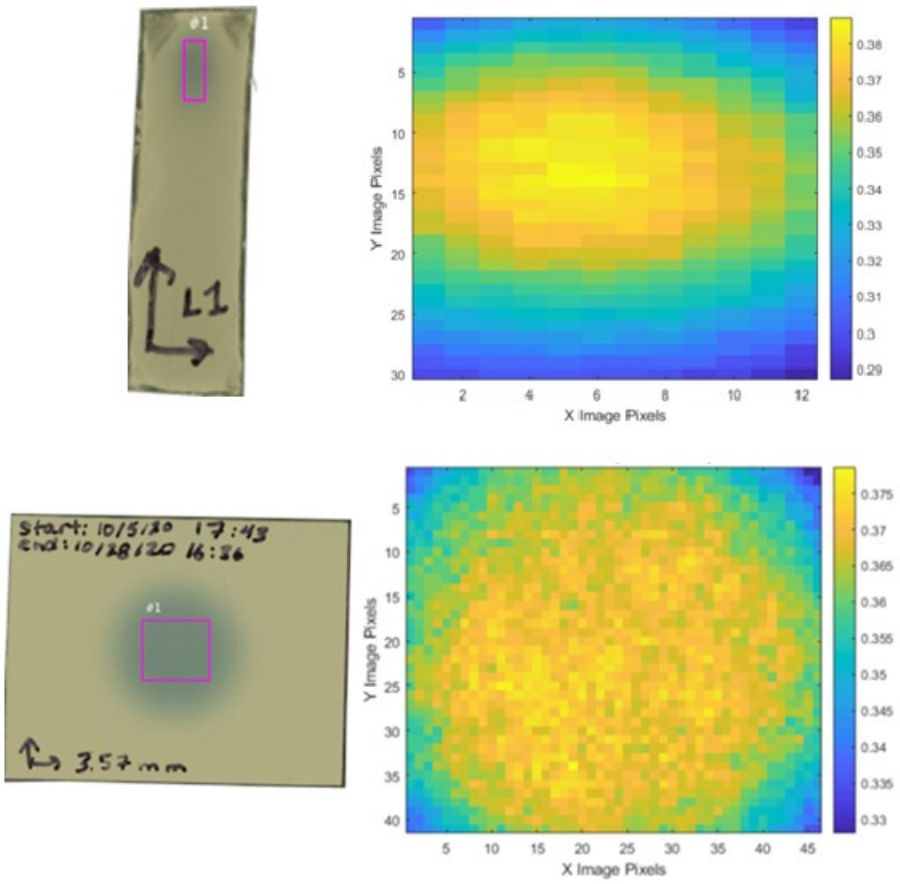

Figure 2. Exposed radiochromic film from the ventral surface of the spinal canal of the L1 vertebra (top left) and from beneath a 3.57-mm-thick sheet of polycarbonate that was placed under a radioactive cylinder (bottom left). The sampled region is indicated by the rectangle on the dark, exposed region of each piece of film. The scanned optical densities for the red channel within the sampled region are shown (top and bottom right). A 3x3 mean filter was applied to these data. Dose was calculated from each color channel and then averaged over all three color channels to obtain the pixel dose. The maximum pixel dose within each sampled region is plotted in **Figures 3-4**.

2.4. In vivo kyphoplasty with ^{32}P brachytherapy bone cement

Six Rambouillet X Columbia ewes, ages 2-3 years, underwent kyphoplasty at the first or second lumbar vertebra, as described below. Three ewes received ^{32}P-HAP mixed with bone cement (experimental sheep) and the other three ewes received non-radioactive HAP mixed with bone cement (control sheep). The activities at the time of implantation into the three experimental sheep were 3.03 mCi/mL, 2.89 mCi/mL, and 2.23 mCi/mL, based on dose calibrator measurements. The protocol was reviewed and approved by the UCI IACUC (AUP-20-046); the UCI animal care and use program is fully accredited by AAALAC International.

The sheep were allowed to acclimate for 10-12 days and were fasted for 12 hours preoperatively. On the day of surgery, gentamicin (3 mg/kg) intramuscularly (IM), penicillin (30,000 IU/kg) IM, glycopyrrolate (0.01 mg/kg) IM, sustained-release buprenorphine (0.1 mg/kg) subcutaneously, and flunixin meglumine (1.1 mg/kg) IM were administered preoperatively. Anesthesia was induced with propofol (7 mg/kg) intravenously, and the sheep were intubated with an endotracheal tube. Isoflurane in 100% oxygen at 2-3% was administered throughout the procedure. Heart rate, end-tidal CO_2, percent O_2 saturation, body temperature, and respiratory rate were monitored continuously. Ceftiofur (2.2 mg/kg) IM and flunixin meglumine (1.1 mg/kg) IM were administered post-operatively and once daily for 3 additional days.

Two surgical approaches were investigated under C-arm visualization, both involving a 5.2 mm diameter drill hole into the cranial portion of the L1 or L2 vertebral body, past the midline, resulting in a cavity at least 15 mm deep. In the first two control sheep, a dorsal approach was used, with a hole drilled through the base of the lateral process, roughly representing percutaneous kyphoplasty in humans. For the three experimental sheep and the final control sheep, a lateral retroperitoneal approach, ventral to the transverse processes, was used to

expose the operative vertebra (Bungartz 2016). After drilling, the hole was then filled completely with bone cement. Routine 2-layer closure was performed. The sheep were monitored closely immediately postoperatively until they were able to stand. They were offered food and checked in the evening. Health checks were performed daily for the three days after surgery, particularly checking for proprioception and motor strength in the rear legs. For the following 6 weeks, general health and gait were evaluated weekly by a veterinarian to ensure that the sheep were walking normally. The animals were sacrificed 23 weeks postoperatively.

The dose rate above the surgical incision was measured just after surgery using an ion chamber (Model # TBM-IC-LR, Technical Associates). Urine and feces were evaluated daily for the presence of radiation (Model 3 Survey Meter, Model 44-9 GM detector, Ludlum Measurements, Inc.). Blood (3 mL) was collected on postoperative days 2, 4, 6, 10, 14, 22, 34, and 42 and tested for radioactivity by placing the sample in a NaI drilled-well scintillation crystal counter (CRC-55t Well Counter, Capintec, Inc.), counting the detected disintegrations over the full spectrum for 10 minutes, and subtracting the detected disintegrations when the well was empty (background counts) to obtain "net counts". Measured activity was calculated by dividing the net counts by the well counter efficiency for ^{32}P in blood. The blood sample was considered to contain activity above the background level if the net counts exceeded the minimum detectable counts (MDC) or, equivalently, if the measured activity exceeded the minimum detectable activity (MDA) (see Appendix).

Erythrocyte sedimentation rate (ESR) and complete blood count (CBC) with differential were obtained on postoperative days 6, 14, 22, and 32. For each type of test, the means and standard deviations in the experimental and control groups were computed at each time point. The range of these means with their respective standard deviations were computed for each

group. Statistical comparisons were not performed because the goal of this pilot study was to obtain means and standard deviations, making the statistical power too low for meaningful comparisons.

3. Results

The ex vivo dosimetry measurements provided the lifetime dose per mCi ^{32}P/mL of cement versus distance for emissions passing through bone and polycarbonate to the radiochromic film (Figures 3-4). The data for nonzero doses were well-fit by curves with exponential decay. Doses were undetectable for distances 5 mm or more from the cement surface in bone and 5.45 mm from the cement surface in polycarbonate after exposing the film for 181 days and 6.8 days from the time the cement was mixed, respectively. The dose that penetrated through 2.5 mm and 4 mm of polycarbonate was, respectively, 13.4 and 3.6 times the dose that penetrated through the same thickness of bone.

All surgeries were completed without complications, with all sheep standing and eating within three to five hours of surgery, and all postoperative physical examinations within normal limits. We found that the lateral retroperitoneal surgical approach was technically easier to perform than the dorsal approach; due to the anatomy of the sheep, the dorsal approach, which was performed on two control sheep, would have caused the distance between the cement and spinal cord to be too small to allow for safe placement of the brachytherapy cement. Therefore, the lateral retroperitoneal approach was performed on one control and all three experimental sheep, which enabled the surface of the brachytherapy cement to be at least 5 mm from nerve roots and the spinal cord.

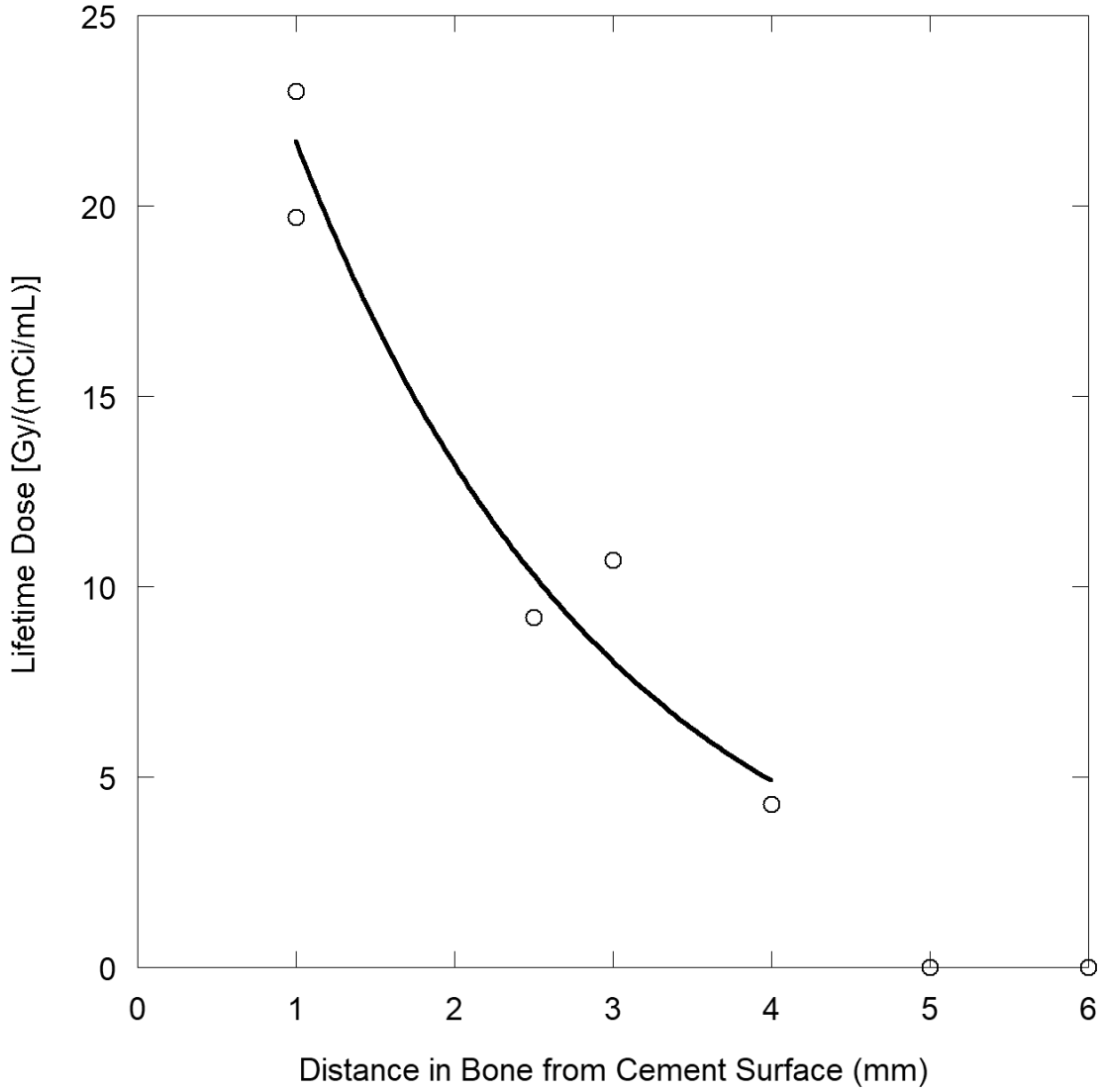

Figure 3. Lifetime dose to radiochromic film at the ventral aspect of the spinal canal, i.e. the approximate lifetime dose that would be delivered to the surface of the spinal cord, versus distance in bone from the surface of the brachytherapy cement. Lifetime Dose [Gy/(mCi/mL)] = $35.6\ e^{(-0.496\ x)}$, where x (mm) is the distance in bone (R=0.971).

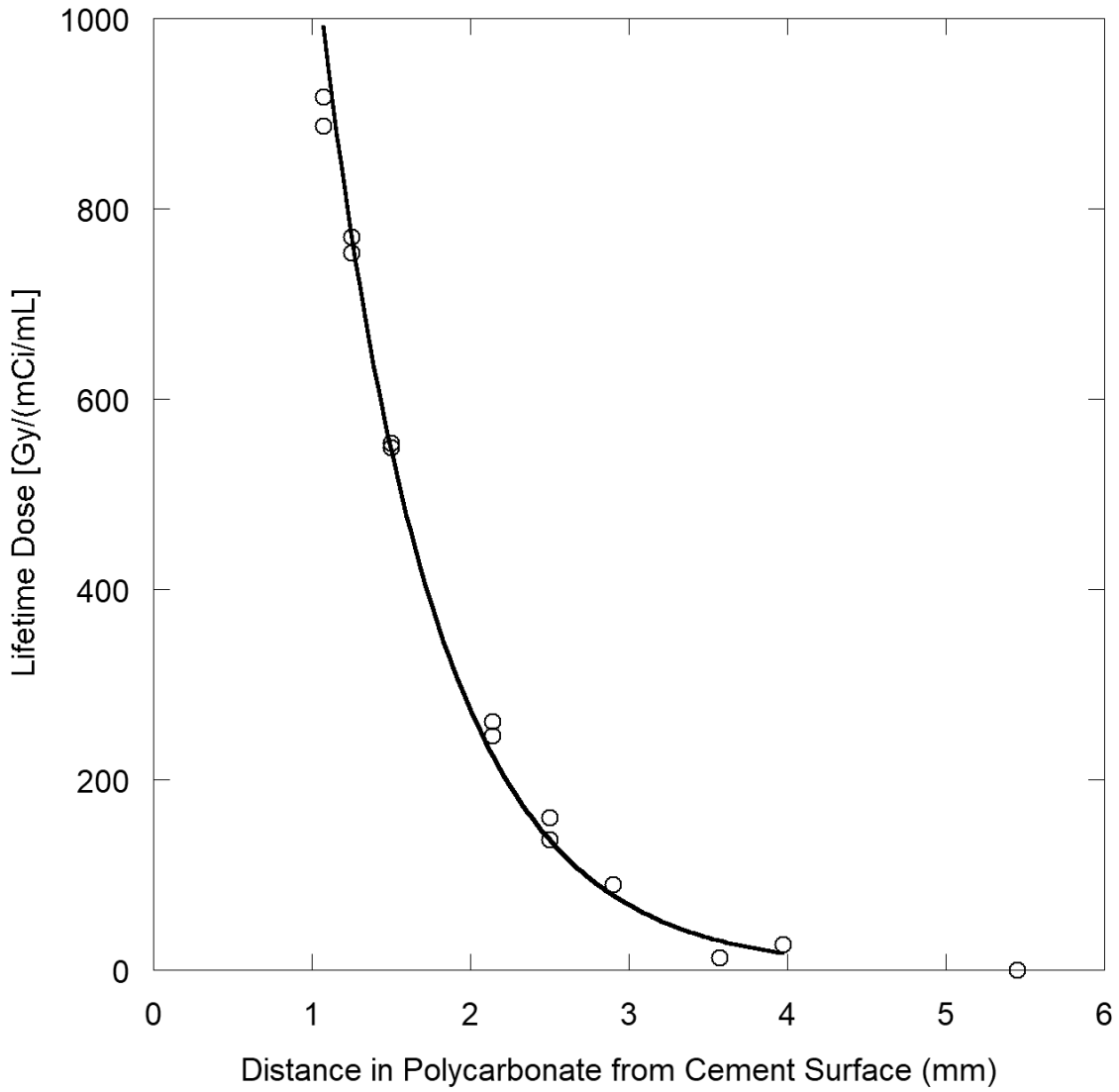

Figure 4. Lifetime dose to radiochromic film versus distance in polycarbonate from the surface of the brachytherapy cement. Lifetime Dose [Gy/(mCi/mL)] = 4350 e $^{(-1.38\ x)}$, where x (mm) is the distance in polycarbonate (R=0.997).

Brachytherapy cement was present in the soft tissue of the first experimental sheep which resulted in measurable amounts of radioactivity on bloodied areas of the skin surface near the incision. Cleaning the area removed the contamination, but the dose rate was not notably reduced. The dose rate in this case was 185 μSv/hr at 5 cm and 30 μSv/hr at 30 cm above the surgical site. In the second surgery, cement was placed only in the vertebra, with no cement in the soft tissue. Adjacent to the incision, emissions were detected using a Geiger-Muller counter, but the dose rate was below detectable levels using the ion chamber (<0.1 μSv/hr). In the third sheep, the dose rate adjacent to the incision was 4 μSv/hr.

Net counts (counts over background) in the blood of the experimental sheep were ≤ 15 cpm, with a median of -13.5 cpm, similar to net counts in the blood of control sheep, ≤ 65 cpm, with a median of 0 cpm (Figure 5). Net counts from the blood of the experimental sheep were below the MDC of 25 cpm to 37 cpm and the MDA of 3.3 Bq/mL to 4.8 Bq/mL, respectively, although the blood of the control sheep demonstrated counts above those levels. Using a Geiger-Muller counter, no activity was detected in the urine or feces of the sheep at any time. CBC with differential and ESR results were unremarkable, with similar results for control and experimental sheep (Table 1).

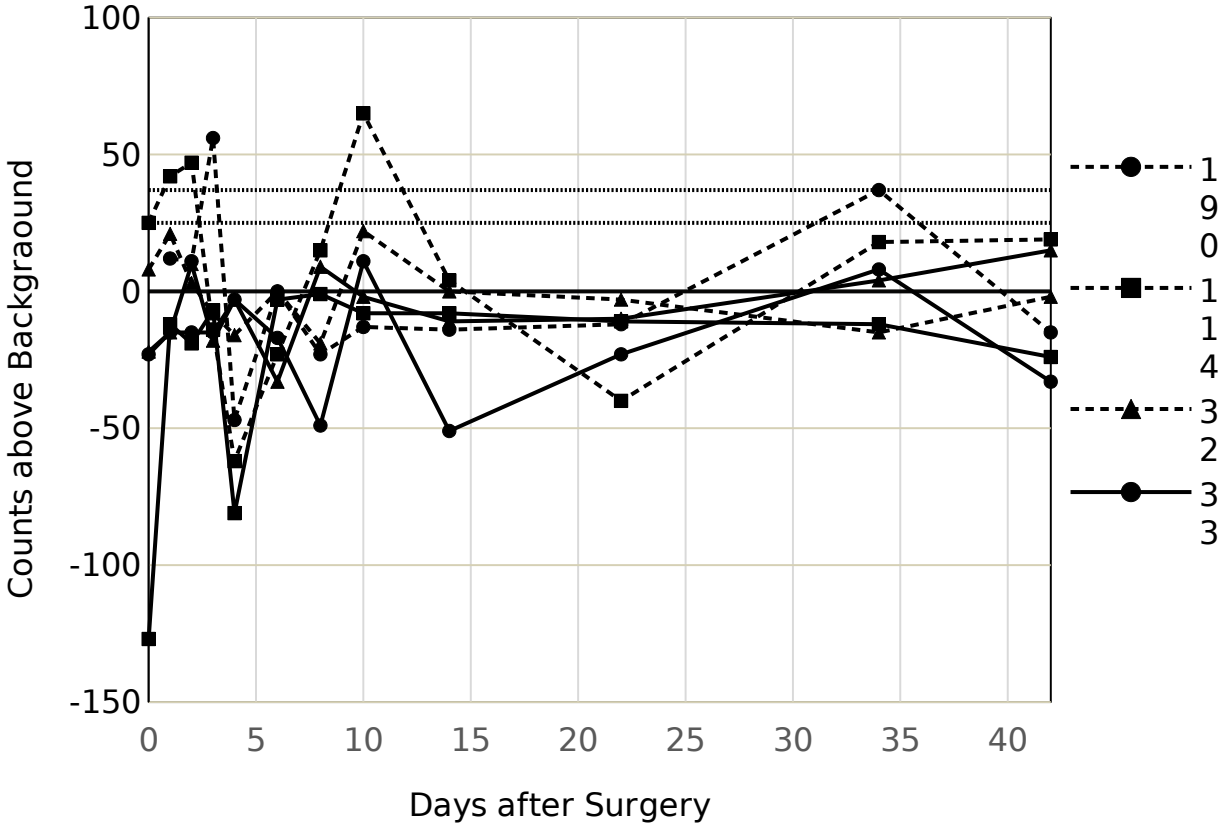

Figure 5. Well counter results for 3 mL of blood drawn from each sheep after surgery. Results for animals that received brachytherapy cement (solid lines) and control animals (dashed lines) may be compared with the threshold for concluding that activity is present, the minimum detectable counts (MDC). The horizontal dotted lines reflect the range of MDC values, 25 cpm to 37 cpm (25 cpm to 29 cpm for the control sheep and radioactive sheep #28; 27 cpm to 37 cpm for sheep #33 and #106). The legend indicates the animal identification numbers.

Table 1. Blood test results. At each time point, mean and standard deviation in each group were calculated. The range of these means over the four time points is presented with the respective standard deviations (SD) in parentheses.

	Lowest Mean (SD) – Highest Mean (SD) Over the Four Time Points	
	Control Group	**Radioactive Group**
White blood cell count (10^3/μL)	5.1 (0.17) – 6.1 (0.85)	5.8 (0.81) – 8.8 (3.50)
Red blood cell count (10^6/μL)	9.0 (0.31) – 10.1 (0.66)	10.0 (2.33) – 10.7 (1.30)
Hemoglobin (g/dL)	10.2 (0.78) – 11.3 (1.02)	10.5 (1.65) – 11.4 (1.65)
Hematocrit (%)	30.7 (2.08) – 35.7 (5.77)	33.0 (7.25) – 36.7 (9.07)
Mean corpuscular volume (fL)	33 (1.2) – 35 (3.1)	31 (1.0) – 35 (5.8)
Mean corpuscular hemoglobin (pg)	11.0 (0.44) – 11.3 (0.55)	10.3 (0.15) – 10.8 (0.21)
Mean corpuscular hemoglobin concentration (g/dL)	31 (0.6) – 34 (0.6)	30 (4.9) – 34 (0.6)
Platelet count (10^3/μL)	475 (25.4) – 893 (196.6)	522 (142.8) – 612 (202.5)
Neutrophils (segmented)	1435 (707.9) – 2421 (1389.3)	2107 (989.3) – 4941 (2928.3)
Neutrophils (bands)	0 (0)	0 (0)
Lymphocytes	2928 (288.1) – 3295 (614.6)	3035 (413.1) – 3534 (1705.2)
Monocytes	154 (138.8) – 318 (78.0)	117 (16.2) – 233 (189.1)
Eosinophils	236 (88.5) – 311 (129.6)	161 (97.6) – 264 (177.5)
Basophils	0 (0)	0 (0)
Eosinophil sedimentation rate (mm/h)	1.0 (1.73) – 7.2 (6.21)	0 (0) – 3.7 (3.79)

4. Discussion

The goal of this study was to answer key questions about ^{32}P brachytherapy bone cement in preparation for future animal studies in vivo. We performed experiments ex vivo to quantify safe distances between the spinal cord and brachytherapy bone cement in the sheep vertebral body and between sensitive soft tissues and brachytherapy bone cement. We also performed a pilot study in vivo to assess the preferred surgical approach, to determine if ^{32}P leaches from the cement into the bloodstream, or is excreted in the urine or feces, and to identify any unexpected adverse effects from the cement that would potentially influence translation of ^{32}P brachytherapy bone cement to clinical use.

Our experimental data for the lifetime dose to the surface of the spinal cord versus distance in bone from the cement surface can be compared with our dose distributions in human trabecular vertebral bone calculated previously using Monte Carlo models. When the cement surface was 1 mm from the ventral aspect of the spinal canal, the measured lifetime dose was just 22 Gy/mCi/mL in sheep compared with 750 Gy/mCi/mL in human bone (Keyak *et al* 2015). This discrepancy is too large to be attributed to the four-fold greater density of ovine trabecular vertebral bone compared with human trabecular vertebral bone (Liebschner 2004) or to the presence of cortical bone in the ovine specimens (Keyak *et al* 2015). Therefore, we attribute this lack of agreement to a modest understatement of distance in a steep portion of the dose-distance curve. Agreement with our previous data was considerably better when the cement surface was 2.5 mm from the ventral aspect of the spinal canal, with a lifetime dose of 10 Gy/mCi/mL, compared with a dose of 20 Gy/mCi/mL in human cortical bone (Keyak *et al* 2015). Given the greater density of sheep trabecular bone and the dense cortex at the ventral aspect of the ovine spinal canal, these doses are in agreement. Finally, placing the cement surface at least 4 mm

from the ovine spinal cord would result in a lifetime dose of less than 5 Gy/mCi/mL, or 15 Gy for the cement used in the in vivo portion of our study which contained up to 3 mCi ^{32}P/mL. This dose is consistent with our previously calculated lifetime dose of 12.5 Gy at a distance of up to 4.7 mm (Kaneko *et al* 2012), considering the greater density of ovine bone. The maximum allowable lifetime dose to the spinal cord from ^{32}P brachytherapy cement is 54 Gy (Kaneko *et al* 2012), so cement with an activity concentration of 4 mCi/mL could be safely implanted in the vertebral body if the surface of the cement is kept at least 4 mm from the spinal cord in sheep and 5 mm from the spinal cord in humans.

The dose from brachytherapy cement in soft tissue is important because cement at the drill hole entrance to the vertebral body will irradiate soft tissues in the area, such as the peripheral nerves. We used polycarbonate to simulate soft tissue in our experiments. Polycarbonate, acrylic, water and soft tissues have similar radiological properties, i.e. linear collision stopping power and scattering power, with similar effective atomic numbers (polycarbonate, 6.36; acrylic, 6.47; water, 7.42) and electron densities (polycarbonate, 3.83×10^{23} electrons/cm^3; acrylic, 3.84×10^{23} electrons/cm^3; water, 3.34×10^{23} electrons/cm^3; muscle, 3.51×10^{23} electrons/cm^3) (Gerbi *et al* 2009, Shrimpton 1981). The effective density of acrylic relative to water, i.e. the ratio of penetration in water to penetration in acrylic, is 1.11 (Loevinger *et al* 1961), so the measured lifetime doses 3 mm and 4 mm from the cement surface in polycarbonate, 69 Gy/mCi/mL and 17 Gy/mCi/mL, respectively, approximate lifetime doses 3.3 mm and 4.4 mm from the cement surface in water. Our previous models simulated bone marrow, not water, but the lifetime doses 3.3 mm, 4.4 mm and 5 mm from the cement surface were 85 Gy/mCi/mL, 20 Gy/mCi/mL and 7 Gy/mCi/mL, respectively (Keyak *et al* 2015). Based on the agreement between our measured and computed doses, we can conclude that brachytherapy

cement with an activity concentration of 4 mCi/mL should be placed no closer than 5 mm from sensitive tissues, such as peripheral nerves.

In our surgical experiments, we found that a lateral retroperitoneal approach, ventral to the transverse processes (Bungartz *et al* 2016) was relatively easy to perform while allowing for a comfortable, safe distance between the surface of the brachytherapy cement and the spinal cord and nerves. We tested for ^{32}P in the bloodstream which, if present in high concentrations, could lead to serious adverse effects. The measured activity in the blood of the experimental sheep was below that of the control sheep and below the MDA of 3.3 Bq/mL to 4.8 Bq/mL even when brachytherapy cement had extravasated into the adjacent soft tissue. If substantial quantities of ^{32}P had been present in the blood, the kidneys would have excreted it in the urine along with stable phosphorus where it would have been detected during radiation surveys of the urine and feces. We also found no evidence of systemic effects associated with radioactivity, which would first present with a decrease in lymphocytes, and we found no sign of inflammation, which would present as elevated ESR. These findings are not surprising because the ^{32}P-HAP was embedded within the bone cement and because hydroxyapatite has very low solubility in water. However, experimental confirmation that there is indeed no detectable activity in the blood and waste is reassuring from a radiation safety standpoint in the context of both animal studies and future patient care. Finally, we also found no neurologic deficits, which is consistent with our ex vivo dosimetry studies and maintaining the cement surface at least 5 mm from the spinal cord.

Percutaneous vertebral augmentation has been previously combined with brachytherapy through use of Samarium-153–ethylene diamine tetramethylene phosphonate (^{153}Sm-EDTMP), a liquid (Ashmalla *et al* 2009, Cardoso *et al* 2009) or by implanting I-125 seeds prior to injecting bone cement. Both approaches deliver a significant dose to the spinal cord due to gamma

emissions from these radioisotopes and require treatment planning to ensure that the spinal cord is not harmed. Unlike I-125 seeds and the ^{32}P-HAP in the present study which remain in the vertebral body, liquid ^{153}Sm-EDTMP is known to leave the bone cement, having been visualized through imaging at distant metastatic sites.

Brachytherapy with I-125 seeds has been the subject of patient studies that have demonstrated pain relief (Lu *et al* 2019, Xie *et al* 2020). However, this treatment may be challenging to perform because the physician must place the individual brachytherapy seeds in the proper locations inside the vertebral body. These locations are determined through treatment planning prior to the procedure to ensure that the desired dose distribution is achieved while not harming the spinal cord.

Our previous dosimetry data can be used to gauge the potential efficacy of brachytherapy cement for treating metastatic tumors in bone (Kaneko *et al* 2012). We reported that an often-prescribed EBRT treatment for patients with spinal metastases (30 Gy delivered over 10 daily treatment sessions of 3 Gy per fraction) would be biologically equivalent to a dose of 38 Gy from a ^{32}P permanent implant. In comparison, brachytherapy cement with an activity concentration of 4 mCi/mL implanted in human bone would deliver over 100 Gy within 2.7 mm to 4.1 mm of the cement surface. Thus, brachytherapy bone cement could deliver a greater dose to regions of the vertebral body than conventional EBRT. Given that the presence of the spinal cord inherently limits the dose that can be delivered by EBRT, IMRT and SBRT, brachytherapy cement could be especially beneficial to patients with radioresistant tumors.

Vertebral augmentation using our brachytherapy cement has advantages beyond simply combining a multi-visit treatment and a minimally invasive surgery into a single procedure. Due to the nature of beta emissions, this treatment would not induce the side effects of conventional

external beam radiation which passes through the skin, gastrointestinal tract, and other tissues. These side effects reduce the patient's quality of life and often prevent them from completing the full course of treatment. Our new treatment would also provide a new option for patients who have already received EBRT and whose tumor did not respond or recurred. These patients currently require more expensive treatments, such as SBRT or IMRT, which have limited availability due to high capitalization requirements. Treatment with brachytherapy cement requires less capital-intensive infrastructure, so it would be more widely available. Using brachytherapy cement as the first treatment would also not preclude subsequent treatment with EBRT, IMRT or SBRT in the event of tumor recurrence. Indeed, the previously implanted brachytherapy cement would continue to reinforce the structure after subsequent external radiotherapy treatments further weaken the remaining bone.

Brachytherapy cement has the potential to significantly improve patient quality of life while keeping the vertebroplasty or kyphoplasty procedure used to implant this cement essentially unchanged. Thus, physicians who perform vertebral augmentation would employ their existing skill set in combination with minimal additional training to treat patients with brachytherapy cement. The dosimetry concepts are simple, requiring sensitive tissues, such as the spinal cord and peripheral nerves, to be kept at least 5 mm from the surface of the cement for an activity concentration of 4 mCi/mL. Brachytherapy cement could also be used with newer technologies, such as radiofrequency ablation (RFA), enabling the macroscopic tumor to be removed and treating adjacent microscopic disease that remains with brachytherapy, while providing immediate pain relief. This approach would be consistent with previous research indicating that optimal results from RFA were obtained only when combined with vertebral augmentation and radiation therapy (Cazzato *et al* 2018).

When using brachytherapy bone cement, the risk of extravasation must be considered and precautions to prevent extravasation should be used. Our previous study showed that, if ^{32}P brachytherapy cement were placed immediately adjacent to the spinal cord and were allowed to remain in place, about 10% and 20% of the spinal cord cross-section would receive lifetime doses greater than 50 Gy/mCi/mL and 10 Gy/mCi/mL, respectively (Kaneko *et al* 2012). Unfortunately, we do not know the effect of continuous beta emissions on a portion of the spinal cord cross-section, but clearly, in the event of extravasation adjacent to the spinal cord, a procedure to remove the extravasated cement must be undertaken as soon as possible. Additionally, as a precaution, patients without an intact posterior cortex should not be considered candidates for this procedure, pending future developments to address the risks of extravasation in this population.

5. Conclusion

The results of this pilot study and our previous dosimetry studies on human bone demonstrate, on a preliminary level, the relative safety of this brachytherapy cement and support additional development and testing. Additional preclinical studies, such as histologic examination of bone near brachytherapy cement, and clinical trials are needed before this promising treatment can be made available to patients with metastatic lesions in the vertebral body.

Appendix. Measurement of ^{32}P activity in ^{32}P-HAP and blood

Cherenkov efficiency

Due to the presence of low-energy β-emitting calcium radioisotopes in the ^{32}P-HAP, we used Cherenkov counting to determine the ^{32}P activity in our ^{32}P-HAP. To obtain the Cherenkov counting efficiency, we first irradiated four vials containing 500 µL each of 0.01 M to 0.6 M phosphoric acid for 1 hr in the lazy Susan of the nuclear reactor located at UCI (TRIGA®, General Atomics) to create ^{32}P. Then, 200 µL of each concentration of phosphoric acid was moved to a plastic vial that was filled with either 3 mL distilled water or 3 mL aqueous scintillation cocktail (Ready Safe, Beckman Coulter) and then counted with a liquid scintillation counter (LSC, LS 6500 Scintillation System, Beckman Coulter) for 10 minutes. We considered the counts with cocktail to be 100% efficient for ^{32}P because ^{32}P is a high-energy β-emitter. Using linear regression analysis, while forcing the line through the origin, we obtained slopes that indicated cpm per mole of phosphorus. The LSC Cherenkov efficiency was then obtained by dividing the slope for Cherenkov counting (5.38×10^9 cpm/mol, R^2=0.99) by the slope for cpm with LSC cocktail (8.86×10^9 cpm/mol, R^2=0.99) to obtain a Cherenkov efficiency of 61%. We also confirmed that the presence of hydroxyapatite did not affect Cherenkov counts in subsequent measurements by performing Cherenkov counting with and without the addition of hydroxyapatite.

Dose Calibrator Calibration

The Calibration Vial containing ^{32}P-HAP was allowed to decay for 111 days and was dissolved in 20 mL 1 M phosphoric acid. Cherenkov counting was then performed on 60 µL of that

solution, corrected for the Cherenkov efficiency, scaled to obtain the total activity in the Calibration Vial at the time of LSC Cherenkov counting, and corrected for decay to determine the Calibration Vial activity at the time of measurement by the dose calibrator (Actual Calibration Vial Activity). A scaling factor, ***s***, to calculate actual vial activities from provisional vial activities measured by the dose calibrator was calculated as

s = (Actual Calibration Vial Activity)/(Provisional Calibration Vial Activity)

Well Counter Efficiency

To evaluate the efficiency of the well counter (CRC®-55tW, Capintec, Inc.) to detect ^{32}P in blood, 22.5 µL of 0.6 M phosphoric acid containing an activity of 750 Bq, or 45013 dpm (measured by LSC with cocktail and adjusted for decay at the time of counting in the well counter) was moved to a 3 mL blood-collection tube, 3 mL sheep blood was added, and this vial was counted over the full spectrum by the well counter for 10 minutes. The number of counts per minute above background measured by the well counter, 1913 cpm, was divided by the actual activity measured by the LSC, 45013 dpm, to obtain the well counter efficiency for ^{32}P in blood, 0.042, or 4.2%. From this efficiency and the number of background counts over the full spectrum (BKG) in 10 minutes, we calculated the minimum detectable counts (MDC) and the minimum detectable activity (MDA) in sheep blood during the in vivo study using the following equations (CRC®-55t Well Counter Owner's Manual, 2017):

$$MDC = \frac{f * \sqrt{BKG(cpm) * T(min)}}{T(min)}$$

$$MDA = \frac{f * \sqrt{BKG(cpm) * T(min)}}{Efficiency * T(min)}$$

where *f* is the precision factor (a value of 3 was used) and T is the counting time (10 min). Background ranged from about 700 to 1500 cpm (the higher values occurred when ^{32}P-HAP from this study was located in the room), resulting in an MDC between 25 cpm and 29 cpm for the control sheep and one of the experimental sheep (#28) and an MDC of 27 cpm to 37 cpm for the remaining experimental sheep (#33 and #106). After accounting for the well counter efficiency of 0.042, the MDA was 600 to 880 dpm in 3 mL of blood, which is equivalent to 3.3 Bq/mL to 4.8 Bq/mL.

Acknowledgements

We gratefully acknowledge funding provided by the UCI Department of Radiological Sciences, UCI Undergraduate Research Opportunities Program, UCI California Institute for Telecommunications and Information Technology, and UCI Foundation. Research reported in this publication was supported in part by the National Cancer Institute of the National Institutes of Health under award number P30CA062203 and the UC Irvine Comprehensive Cancer Center using UCI Anti-Cancer Challenge funds. The content is solely the responsibility of the authors and does not necessarily represent the official views of the National Institutes of Health or the Chao Family Comprehensive Cancer Center.

We are grateful to members of the UCI Radiation Safety Division and University Laboratory Animal Resources who helped make this challenging study possible. We thank McClellan Nuclear Research Center, University of California, Davis, and Jack Hamilton, C6 Systems, Inc. for their assistance.

CRediT authorship contributions: Joyce H. Keyak (all aspects of study) – Conceptualization, Formal Analysis, Funding acquisition, Investigation, Methodology, Project

Administration, Resources, Software, Supervision, Validation, Visualization, Writing – original draft, Writing – review & editing; Mando L. Eijansantos (in vivo and ex vivo aspects of study) – Investigation, Methodology, Software, Validation. Writing – original draft, Writing – review & editing; Katherine G. Rosecrance (ex vivo dosimetric analysis) – Formal Analysis, Methodology, Software, Supervision, Validation, Visualization, Writing – original draft, Writing – review & editing; Daniel Wong (designing/fabricating devices for mixing cement, ex vivo dosimetric analysis) – Formal Analysis, Methodology, Resources, Software, Validation, Visualization, Writing – review & editing; Sayeh Feizi (designing/fabricating devices for mixing cement) – Resources, Writing – review & editing; Aleen L. Meldosian (ex vivo dosimetric analysis) – Formal Analysis, Methodology, Software, Validation, Visualization, Writing – review & editing; Pranav Peddinti (designing/fabricating devices for mixing cement) – Resources, Writing – review & editing; Clifford M. Les (veterinary/surgical aspects of study) – Investigation, Methodology, Resources, Writing – review & editing; Harry B. Skinner (medical/surgical aspects of study) – Conceptualization, Investigation, Methodology, Resources, Writing – review & editing; Varun Sehgal (in vivo and ex vivo medical physics) – Conceptualization, Investigation, Methodology, Resources, Supervision, Writing – review & editing.

Dr. Keyak, Dr. Skinner and Dr. Sehgal are inventors of brachytherapy bone cement, United States Patent Numbers 9,028,499, 9,198,989, 9,597,427 and 10,272,173, and are stockholders in Bone-Rad Therapeutics, Inc. which has licensed these patents.

Data Availability Statement

The data that support the findings of this study are available upon reasonable request from the authors.

References

Ashamalla H, Cardoso E, Macedon M, Guirguis A, Weng L, Ali S, Mokhtar B, Ashamalla M, Panigrahi N. Phase I trial of vertebral intracavitary cement and samarium (VICS): novel technique for treatment of painful vertebral metastasis. Int J Radiat Oncol Biol Phys. 2009 Nov 1;75(3):836-42. https://doi.org/10.1016/j.ijrobp.2008.11.060.

Barzilai, O., Boriani, S., Fisher, C.G., Sahgal, A., Verlaan, J.J., Gokaslan, Z.L., Lazary, A., Bettegowda, C., Rhines, L.D., Laufer, I. (2019). Essential Concepts for the Management of Metastatic Spine Disease: What the Surgeon Should Know and Practice. *Global Spine Journal, 9,* 98-107. https://doi.org/11.1177/2192568219830323

Berenson, J., Pflugmacher, R., Jarzem, P., Zonder, J., Schechtman, K., Tillman, J.B., Bastian, L., Ashraf, T., Brionis, F. (2011). Balloon kyphoplasty versus non-surgical fracture management for treatment of painful vertebral body compression fractures in patients with cancer: a multicentre, randomised controlled trial. *The Lancet Oncology, 12(3),* 225-235. https://doi.org/10.1016/S1470-2045(11)70008-0

Budczies, J., von Winterfeld, M., Klauschen, F., Bockmayr, B., Lennerz, J.K., Denkert, C., Wolf, T., Warth, A., Dietel, M., Anagnostopoulos, I., Weichert, W., Wittschieber, D., Stenzinger, A. (2014). The landscape of metastatic progression patterns across major human cancers. *Oncotarget, 6(1),* 570-583. https://doi.org/10.18632/oncotarget.2677

Bungartz, M., Maenz, S., Kunisch, E., Horbert, V., Xin, L., Gunnella, F., Mika, J., Borowski, J., Bischoff, S., Schubert, H., Sachse, A., Illerhaus, B., Gunster, J., Bossert, J., Jandt, K.D., Kinne, R.W., Brinkmann, O. (2016). First-time systematic postoperative clinical assessment of a minimally invasive approach for lumbar ventrolateral vertebroplasty in the large animal model sheep. *The Spine Journal* 16:1263-1275. https://doi.org/10.1016/j.spinee.2016.06.015

Cardoso E.R., Ashamalla H., Weng L., Mokhtar B., Ali S., Macedon M., Guirguis A. Percutaneous tumor curettage and interstitial delivery of samarium-153 coupled with kyphoplasty for treatment of vertebral metastases. J Neurosurg Spine. 2009 Apr;10(4):336-42. https://doi.org/10.3171/2008.11.SPINE0856.

Cazzato, R.L., Garnon, J., Caudrelier, J., Rao, P.P., Koch, G., Gangi, A. (2018). Percutaneous radiofrequency ablation of painful spinal metastasis: a systematic literature assessment of analgesia and safety. *International Journal of Hyperthermia, 34(8),* 1272-1281. https://doi.org/10.1080/02656736.2018.1425918

CRC®-55t Well Counter Owner's Manual, Manual Stock No. 9250-0138, Rev. K, May 4, 2017, p. 8-21.

EBT3 Specification and User Guide. Available at http://www.gafchromic.com/documents/EBT3_Specifications.pdf

Georgy, B.A. (2008). Metastatic Spinal Lesions: State-of-the-Art Treatment Options and Future Trends. *American Journal of Neuroradiology, 29,* 1605-16011. https://doi.org/10.3174/ajnr.A1137

Gerbi BJ, Antolak JA, Deibel FC, Followill DS, Herman MG, Higgins PD, Huq MS, Mihailidis DN, Yorke ED, Hogstrom KR, Khan FM. Recommendations for clinical electron beam dosimetry: supplement to the recommendations of Task Group 25. Med Phys. 2009 Jul;36(7):3239-79. doi: 10.1118/1.3125820. Erratum in: Med Phys. 2011 Jan;38(1):548. PMID: 19673223.

Hage, W.D., Aboulafia, A.J., Aboulafia, D.M. (2000). Incidence, Location, and Diagnostic Evaluation of Metastatic Bone Disease. *Orthopedic Clinics of North America, 31(4),* 515-528. https://doi.org/10.1016/s0030-5898(05)70171-1

Harel, R., Angelov, L. (2010). Spine metastases: Current treatments and future directions. *European Journal of Cancer, 46*, 2696-2707. https://doi.org/10.1016/j.ejca.2010.04.025

Hernandez, R.K., Wade, S.W., Reich, A., Pirolli, M., Liede, A., Lyman, G.H. (2018). Incidence of bone metastases in patients with solid tumors: analysis of oncology electronic medical records in the United States. *BMC Cancer, 18(1),* 44. https://doi.org/10.1186/s12885-017-3922-0

Husain, Z. A., Sahgal, A., De Salles, A., Funaro, M., Glover, J., Hayashi, M., Hiraoka, M., Levivier, M., Ma, L., Martínez-Alvarez, R., Paddick, J. I., Régis, J., Slotman, B. J., Ryu, S. (2017). Stereotactic body radiotherapy for de novo spinal metastases: systematic review. Journal of neurosurgery. Spine, 27(3), 295–302. https://doi.org/10.3171/2017.1.SPINE16684

Kaneko, T.S., Sehgal, V., Skinner, H.B., Al-Ghazi, M.S.A.L., Ramsinghani, N.S., Keyak, J.H. (2010). Evaluation of a radiation transport modeling method for radioactive bone cement. *Physics in Medicine and Biology, 55,* 2451-2463. https://doi.org/10.1088/0031-9155/55/9/002 Epub 2010 Apr 6. Erratum in: Phys Med Biol. 2012 Nov 7;57(21):7225. PMID: 20371905.

Kaneko, T.S., Sehgal, V., Skinner, H.B., Al-Ghazi, M.S.A.L., Ramsinghani, N.S., Marquez Miranda, M., Keyak, J.H. (2012). Radioactive bone cement for treatment of spinal metastases: a

dosimetric analysis of simulated clinical scenarios. *Physics in Medicine and Biology, 57,* 4387-4401. https://doi.org/10.1088/0031-9155/57/13/4387

Keyak, J.H., Kaneko, T.S., Skinner, H.B., Sehgal, V. (2015) Radioactive Bone Cement. United States Patent No. 9,198,989.

Liebschner, M.A. (2004) Biomechanical considerations of animal models used in tissue engineering of bone. Biomaterials 25: 1697-1714. https://doi.org/10.1016/S0142-9612(03)00515-5

Loevinger, R., Karzmark, C.J., Weissbluth, M. (1961). Radiation therapy with high-energy electrons. Part I. Physical Considerations, 10 to 60 Mev. *Radiology* 77(6), 906-927, p. 922. https://doi.org/10.1148/77.6.906

Lu, C. W., Shao, J., Wu, Y. G., Wang, C., Wu, J. H., Lv, R. X., Ding, M. C., Shi, Z. C., Mao, N. F. (2019). Which Combination Treatment Is Better for Spinal Metastasis: Percutaneous Vertebroplasty With Radiofrequency Ablation, 125I Seed, Zoledronic Acid, or Radiotherapy?. American journal of therapeutics, 26(1), e38–e44. https://doi.org/10.1097/MJT.0000000000000449

Mendel, E., Bourekas, E., Gerszten, P., Golan, J.D. (2009) Percutaneous Techniques in the Treatment of Spine Tumors: What are the diagnostic and therapeutic indications and outcomes? *Spine, 34(22)*, 93-100. https://doi.org/10.1097/brs.0b013e3181b77895

Micke, A., Lewis, D. F., Yu, X. (2011). Multichannel film dosimetry with nonuniformity correction. Medical physics, 38(5), 2523–2534. https://doi.org/10.1118/1.3576105

Palmer, A. L., Bradley, D., Nisbet, A. (2014). Evaluation and implementation of triple-channel radiochromic film dosimetry in brachytherapy. Journal of applied clinical medical physics, 15(4), 4854. https://doi.org/10.1120/jacmp.v15i4.4854

Rich, S. E., Chow, R., Raman, S., Liang Zeng, K., Lutz, S., Lam, H., Silva, M. F., Chow, E. (2018). Update of the systematic review of palliative radiation therapy fractionation for bone metastases. Radiotherapy and oncology : journal of the European Society for Therapeutic Radiology and Oncology, 126(3), 547–557. https://doi.org/10.1016/j.radonc.2018.01.003

Rose, P. S., Laufer, I., Boland, P. J., Hanover, A., Bilsky, M. H., Yamada, J., Lis, E. (2009). Risk of fracture after single fraction image-guided intensity-modulated radiation therapy to spinal

metastases. Journal of clinical oncology : official journal of the American Society of Clinical Oncology, 27(30), 5075–5079. https://doi.org/10.1200/JCO.2008.19.3508

Sahgal, A., Weinberg, V., Ma, L., Chang, E., Chao, S., Muacevic, A., Gorgulho, A., Soltys, S., Gerszten, P. C., Ryu, S., Angelov, L., Gibbs, I., Wong, C. S., Larson, D. A. (2013). Probabilities of radiation myelopathy specific to stereotactic body radiation therapy to guide safe practice. International journal of radiation oncology, biology, physics, 85(2), 341–347. https://doi.org/10.1016/j.ijrobp.2012.05.007

Shrimpton PC. Electron density values of various human tissues: in vitro Compton scatter measurements and calculated ranges. Phys Med Biol. 1981 Sep;26(5):907-11. doi: 10.1088/0031-9155/26/5/010. PMID: 7291311.

Virk, M.S., Han, J.E., Reiner, A.S., McLaughlin, L.A., Sciubba, D.M., Lis, E., Ymada, Y., Bilsky, M., Laufer, I. (2017). Frequency of symptomatic vertebral body compression fractures requiring intervention following single-fraction stereotactic radiosurgery for spinal metastases. *Neurosurgical Focus, 42(1).* https://doi.org/10.3171/2016.10.FOCUS16359

Wong, D.A., Fornasier, V.L., MacNab, I. (1990) Spinal Metastases: The Obvious, the Occult, and the Impostors. *Spine, 15(1),* 1-4. https://doi.org/10.1097/00007632-199001000-00001

Xie LL, Chen XD, Yang CY, Yan ZL, Zhu J, Quan KQ, Pu D. (2020) Efficacy and complications of ^{125}I seeds combined with percutaneous vertebroplasty for metastatic spinal tumors: A literature review. *Asian J Surg*, 43(1):29-35. https://doi.org/10.1016/j.asjsur.2019.05.012

Zeng, K. L., Tseng, C. L., Soliman, H., Weiss, Y., Sahgal, A., Myrehaug, S. (2019). Stereotactic Body Radiotherapy (SBRT) for Oligometastatic Spine Metastases: An Overview. Frontiers in oncology, 9, 337. https://doi.org/10.3389/fonc.2019.00337